Effect of deposition temperature on the electrochromic properties of WO_3 grown by LPCVD

D. Louloudakis[1*], D. Vernardou[1,2], G. Papadimitropoulos[3], D. Davazoglou[3] and E. Koudoumas[1,2]

[1]*Center of Materials Technology and Photonics, School of Engineering, Technological Educational Institute of Crete, 710 04 Heraklion, Crete, Greece*
[2]*Department of Electrical Engineering, School of Engineering, Technological Educational Institute of Crete, 710 04 Heraklion, Crete, Greece*
[3]*NCSR "Demokritos", Institute of Nanoscience and Nanotechnology, P.O. Box 60228, 15310 Agia Paraskevi, Athens, Greece*

*Corresponding author

DOI: 10.5185/amlett.2018.1823
www.vbripress.com/aml

Abstract

Monoclinic electrochromic tungsten trioxide (WO_3) layers were grown on FTO substrates using a Low Pressure Chemical Vapor Deposition (LPCVD) system. The effect of the deposition temperature on the structural and morphological characteristics as well as the electrochromic response of the layers was examined. It was found that increasing deposition temperature improves the crystallinity of the layers which affects their electrochemical/electrochromic behavior. Copyright © 2018 VBRI Press.

Keywords: LPCVD, Tungsten trioxide, Electrochromic response.

Introduction

In recent years, chromic metal oxide layers have attracted scientific interest due to the many technological applications they may be used. For example, vanadium pentoxide (V_2O_5) can be employed in electrochromic smart windows [1], Li+ Batteries [2-3] etc. Similarly, vanadium dioxide (VO_2) has the ability to undergo a phase transition from insulator to metal state at a critical temperature (Tc), a property that can be used in thermochromic smart windows [4-6], optical switches [7], actuator etc. Regarding tungsten trioxide (WO_3) seems to be a rather promising material that can be used in many valuable applications such as photocatalytic coatings [8], batteries [9], sensors [10], capacitors [11] and electrochromic smart windows [12].

During the years, many deposition technics has been used for the development of WO_3 layers with significant electrochromic performance. Sputtering [13-14], pulsed laser deposition (PLD) [15], hydrothermal growth [8] and chemical vapor deposition (CVD) [16-20] are some of them, emphasis given in most of the cases on the study of the effect of deposition parameters on characteristics of the grown layers.

In this work, a low pressure chemical vapor deposition (LPCVD) system has been employed for the development of WO_3 on FTO substrates, using tungsten hexacarbonyl ($W(CO)_6$) as precursor. X-ray diffraction (XRD), Raman spectroscopy, field-emission scanning electron microscopy (FE-SEM) and cyclic voltammetry were used for the characterization of the samples, emphasis given on the effect of the deposition temperature on the basics characteristics and the electrochromic behaviour of the WO_3 layers.

Experimental

The tungsten trioxide layers were deposited on FTO substrates (Pilkington, United Kingdom) using a low pressure chemical vapor deposition system. Tungsten hexacarbonyl ($W(CO)_6$) (Sigma Aldrich, United Kingdom) was used as tungsten precursor without further purification. Finally, the growth was assisted with N_2 (99.999%) and O_2 (99.999%).

The growth of WO_3 was performed in horizontal cold wall reactor [21], the $W(CO)_6$ vapors generated in a bubbler maintained at 80 ^oC and introduced in the reactor at a constant flow of 50 sccm N_2 carrier gas (99.999%). The respective O_2 flow rate through the reactor was kept also constant at 50 sccm, while, the deposition temperature was varied from 350 ^oC to 550 ^oC. Prior to deposition, all substrates were ultrasonically cleaned with propanol, acetone, ultrapure H_2O and dried with N_2.

Structural analysis was performed in a Siemens D5000 X-Ray Diffractometer (using as operating conditions: CuKα with λ = 1.54056 Å, 2θ= 20.0-30.0^o,

step time 60 s/o) and a Nicolet Almega XR micro-Raman system for the range of 100 - 1000 cm^{-1} and a laser excitation at 473 nm. The morphological characteristics of the samples were evaluated in a JEOL JSM-7000F field-emission scanning electron microscope (FE-SEM), after their over-coating with gold, needed to avoid charging. The transmittance measurements were performed in a Perkin Elmer Lambda 950 spectrophotometer over the wavelength range of 300-800 nm. Finally, a three-electrode cell was used for the electrochemical analysis of the samples as reported previously [22-25], employing 1 M $LiClO_4$ in propylene carbonate as the electrolyte. The reference electrode was Ag/AgCl, the counter electrode was Pt and the working electrode was the WO_3 layers on FTO substrates. The measurements were performed using a scan rate of 10 mV s^{-1} in the voltage range of -1000 mV to +1000 mV, the area of the working electrode (WO_3 on FTO) exposed to the electrolyte being 1 cm^2. Chronoamperometry measurements were used to evaluate the lithium ion intercalation / deintercalation process with respect to time, at −1000 mV and +1000 mV for a step of 200 s and a total time period of 1500 s. Finally, the thickness of the layers was determined using an A-step TENCOR profilometer. Prior to these measurements, a step was formed by etching the WO_3 coatings off the FTO glass substrate with 1:3, H_2O_2 (30%):HCl. FTO remained intact after this procedure and the thickness was deduced from the measured step height. The thickness of the coatings deposited at 350 ºC was found <20nm, while for the depositions at 450 and 550 ºC was about 50 nm.

Results and discussion

All as-grown WO_3 layers were uniformly transparent in the visible and appeared to have sufficient adhesion, passing the Scotch tape test (removal of an X shaped piece with sticking tape [5]). Moreover, they had similar properties after six months in air, indicating their stability with time.

Fig. 1 shows the XRD patterns of layers deposited at three different temperatures, 350, 450 and 550 ºC. As can be seen, there is a trend of better crystallinity as the deposition temperature increases.

Fig. 1(a) shows the XRD for the layer deposited at 350 ºC, where there is only one peak at 26.6º which is attributed to the FTO substrate [26] with Miller indices (110), indicating that the WO_3 layers at 350 ºC are amorphous. As the deposition temperature increases, there is a clear improvement of the crystallinity. For the deposition at 450 ºC **(Fig. 1(b))**, the characteristics peaks of monoclinic WO_3 at 23.3 º, 23.8 º, 24.5 º and 28.9 º exist, corresponding to Miller indices (002), (020), (200) and (112) [27-29], with a preferred orientation along (002). Further increase of the deposition temperature up to 550 ºC improved more the crystallinity. As shown in **Fig. 1(c),** the intensity of the peaks have increased and the preferred orientation has changed from (002) to (020).

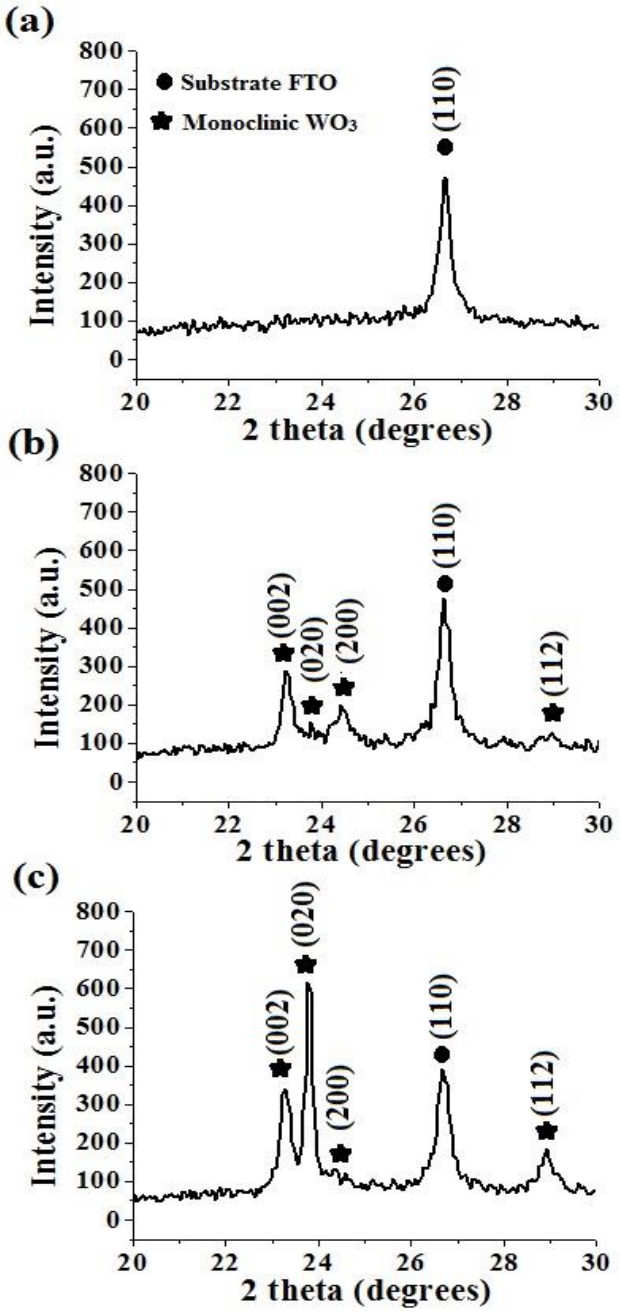

Fig. 1. XRD patterns of the WO_3 layers grown at various deposition temperatures: 350ºC (a) 450ºC (b) and 550ºC (c).

Fig. 2 shows the Raman spectra of the same samples. Raman peaks at the frequencies of 269 and 323 cm^{-1} are assigned the W-O-W bending modes of bridging oxide ions [30], while the W-O-W stretching mode (tungsten oxide network) corresponds to the high frequency Raman peaks at 713 and 806 cm^{-1} [30-31].

In agreement with the XRD results, Raman Spectroscopy reveals a trend towards improved crystallization as the deposition temperature increases, since not only the intensity of the peaks increases, but also these become narrower. Moreover, the spectrum of the samples grown at 350 ºC indicates that this is rather amorphous.

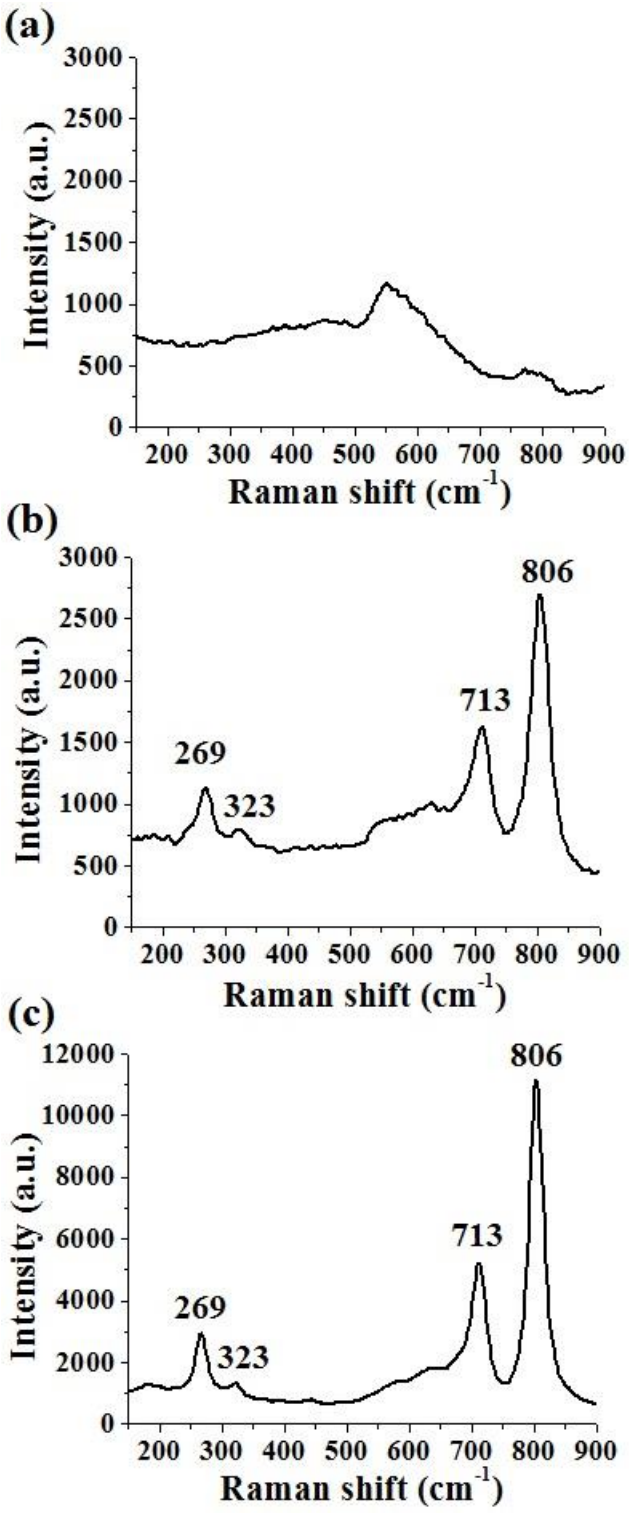

Fig. 2. Raman spectra of WO_3 layers grown at various deposition temperatures: 350ºC (a) 450ºC (b) and 550ºC (c)

Following the morphological characterization, it seems that the change of the preferred orientation can affect the morphology of the layers. As shown in the SEM images of **Fig. 3,** all layers appear to have a granular morphology. Nevertheless, there is a slight change in the morphology structures as the deposition temperature increases.

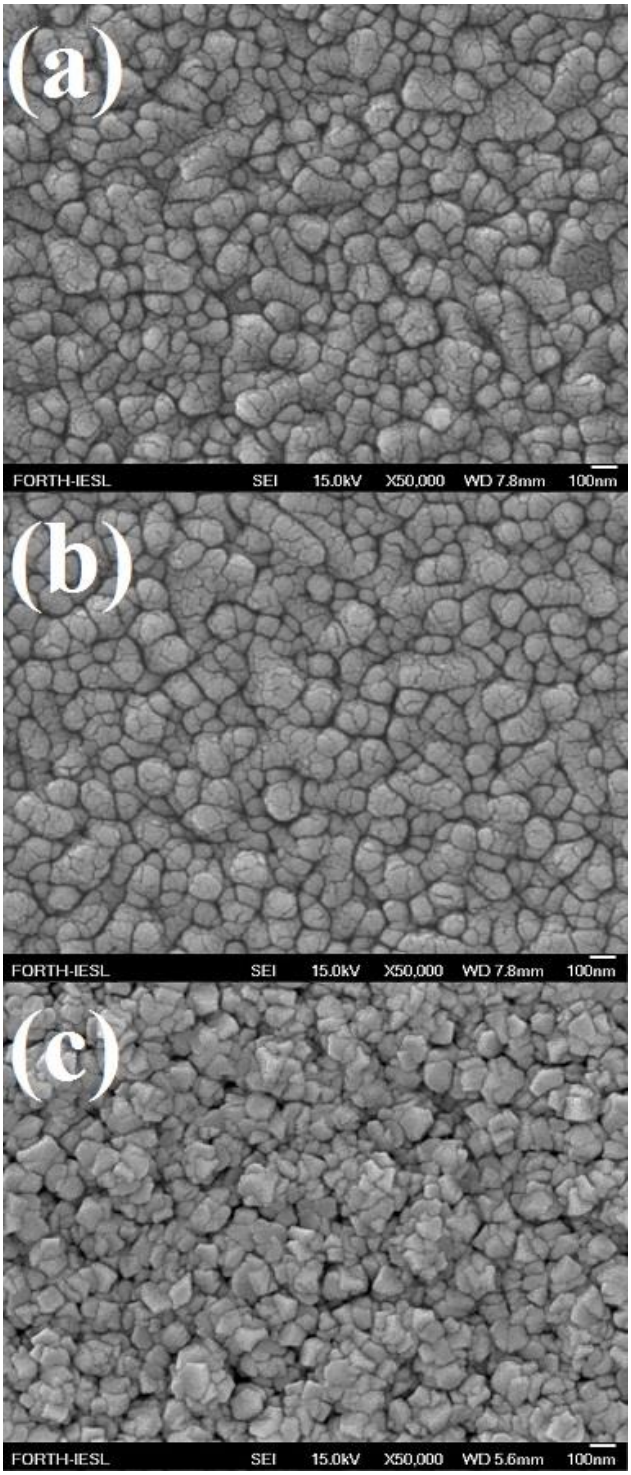

Fig. 3. FE-SEM images of the WO_3 layers grown at various deposition temperatures: 350ºC (a) 450ºC (b) and 550ºC (c)

At 450 ºC the structures are smooth, while, when the deposition temperature increases to 550 ºC, the structures are sharper and their surface becomes more porous. This change in the morphology can be attributed to the change of the preferred orientation, shown in the XRD measurements, because of the strain induced at the (020) plane with increasing temperature, leading in a preferable grow along (020) plane [32].

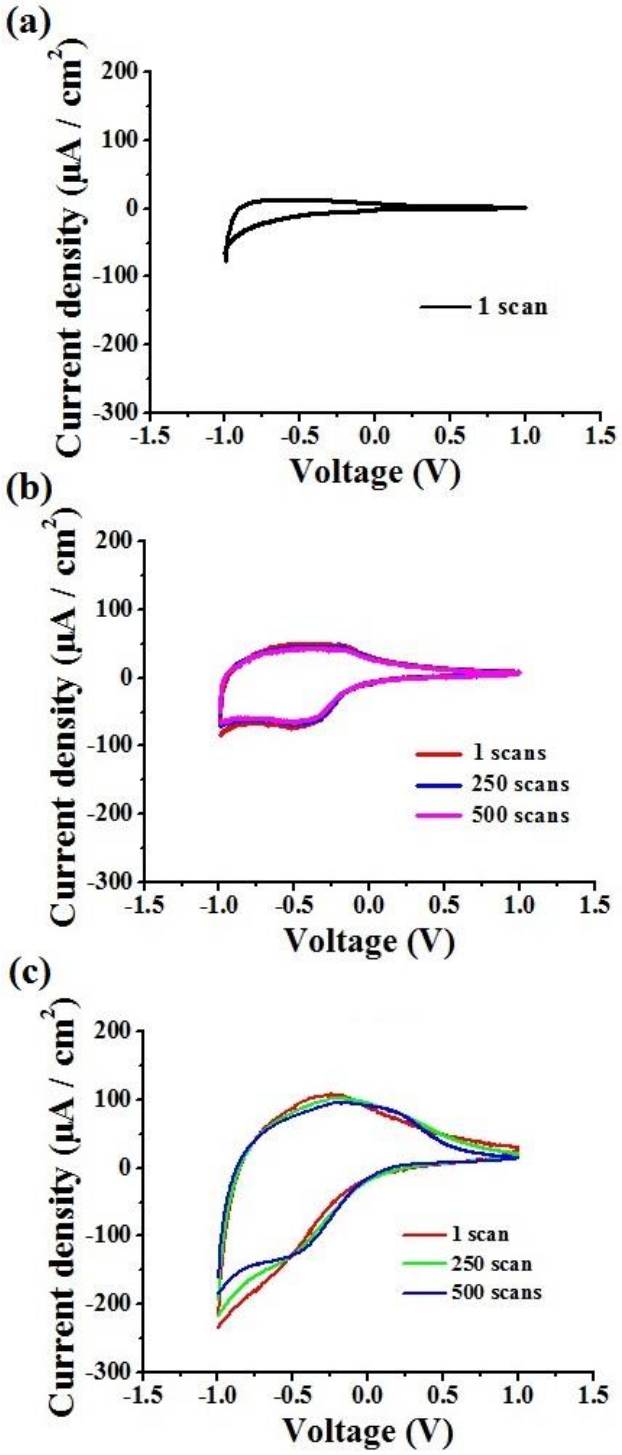

Fig. 4. Cyclic voltammograms of the WO_3 layers grown at various deposition temperatures: 350ºC (a) 450ºC (b) and 550ºC (c), for number of scans 1, 250 and 500, using a scan rate of 10 mV s^{-1} and 1 M $LiClO_4$/propylene carbonate as electrolyte.

In order to evaluate the effect of deposition temperature on the electrochemical performance of the as-grown WO_3 layers, current-voltage curves were recorded for up to 500 scans using the three electrode cell, sweeping the potential between -1000 and +1000 mV at a scan rate of 10 mV s^{-1}, the respective results shown in **Fig. 4**.

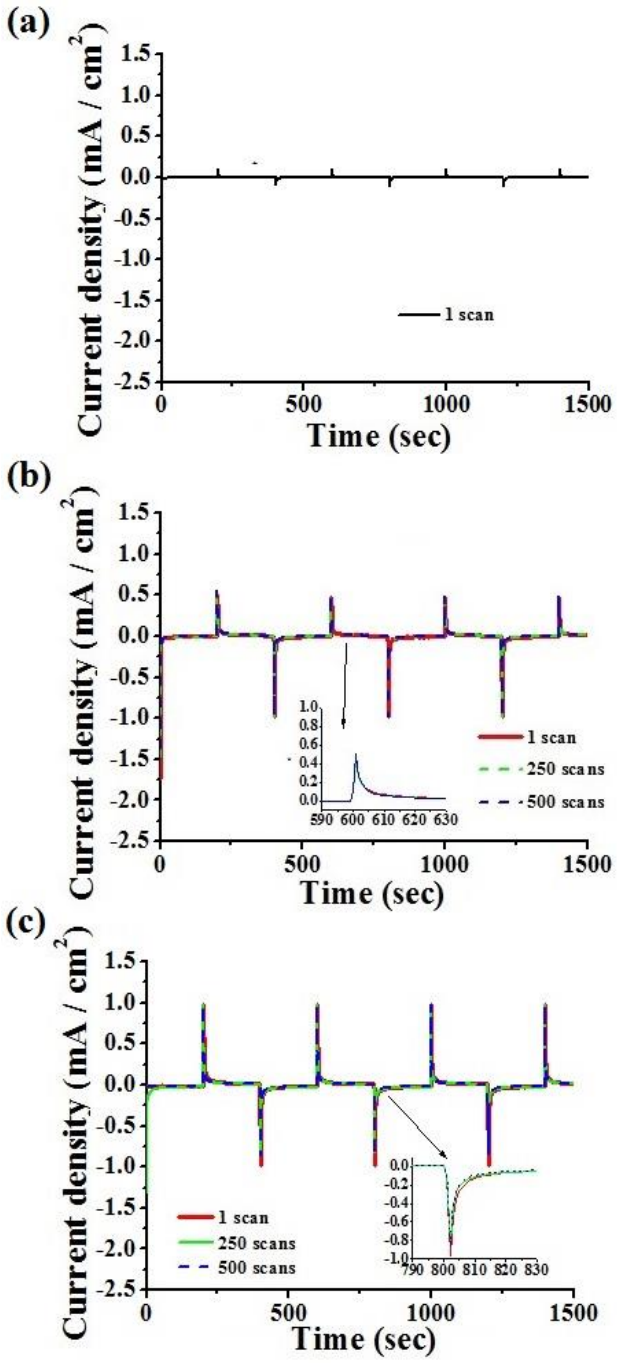

Fig. 5. Current density versus time of the WO_3 layers grown at various deposition temperatures: 350ºC (a) 450ºC (b) and 550ºC (c), at a voltage step of -1000 mV and +1000 mV for an interval of 200 s and total time period of 1500 s up to 500 scans.

The IV curves were normalized to the geometric area of the sample resulting in units of μA / cm^2.

The initially transparent WO_3 layers were turned to blue when they were cathodically polarized in $LiClO_4$, while they became transparent again when anodically polarized. The color - bleach process can be represented according to the following equation [33]:

$$WO_3 \text{ (transparent)} + xLi^+ + xe^- \leftrightarrow Li_xWO_3 \text{ (blue)}$$

500 scans were conducted only for the samples deposited at higher temperatures. For layers deposited at 350 ºC, the current density was found decreasing rapidly after the first scan, because of the amorphous nature of the material. The layers deposited at 450 ºC showed very good stability up to 500 cycles. Finally, although the 550 ºC sample showed an increased current, a shift of the oxidation-reduction reaction peaks and a decrease of the current density was observed after long-term cycling. This indicates that trapping of charge appears as a result of irreversible chemical reactions between the lattice and the Li^+ ions, the amount of the incorporated charge decreasing during the cycling [34-35].

Chronoamperometry measurements were also conducted up to 500 scans and are shown in **Fig. 5**. Using these results, the intercalation charge density (obtained by the integration of the excess current density) and the time response (defined as the time needed for excess current density to reduce by 10% of the absolute maximum value) were calculated [36-37], for the samples under investigation and summarized at **Table 1**. These values indicate that the intercalation charge density is higher for the deposition at 550 ºC which can be attributed to the more porous surface according to the SEM images. However, the deposition at 450 ºC presents a better performance since the difference between intercalation and deintercalation charge density after the first scan is only 7.5%, while for the deposition at 550 ºC this difference approaches 41%. Moreover, after 250 scans, the intercalation charge density was reduced by 16% in the 450 ºC case, while the reduction approaches 25% for the samples deposited at 550 ºC.

Table 1. The investigation of intercalation charge and the time response for the samples.

Growth temperature(ºC)	Intercalation time (s)		De-intercalation time (s)		Intercalation charge (mC/cm^2)		De-intercalation charge (mC/cm^2)	
	1 scan	After 250 scans	1 scan	After 250 scans	1 scan	After 250 scans	1 scan	After 250 scans
350	120	--	120	--	0.59	--	0.24	--
450	13	12	7	6	4.11	3.45	3.80	2.45
550	17	14	10	12	5.17	3.90	3.03	1.97

According to reports in the literature, nanostructured porous WO_3 films have high surface area, which could better facilitate the intercalation/deintercalation of Li-ions into/out of the WO_3 crystal lattice [38]. However, at the same time, there are more trapped ions into the lattice after each cycle, which favors a degradation in the performance.

Fig. 6 shows the ex-situ optical transmission data for the as grown WO_3 layers in the colored and bleached state for the depositions at 450 and 550ºC.

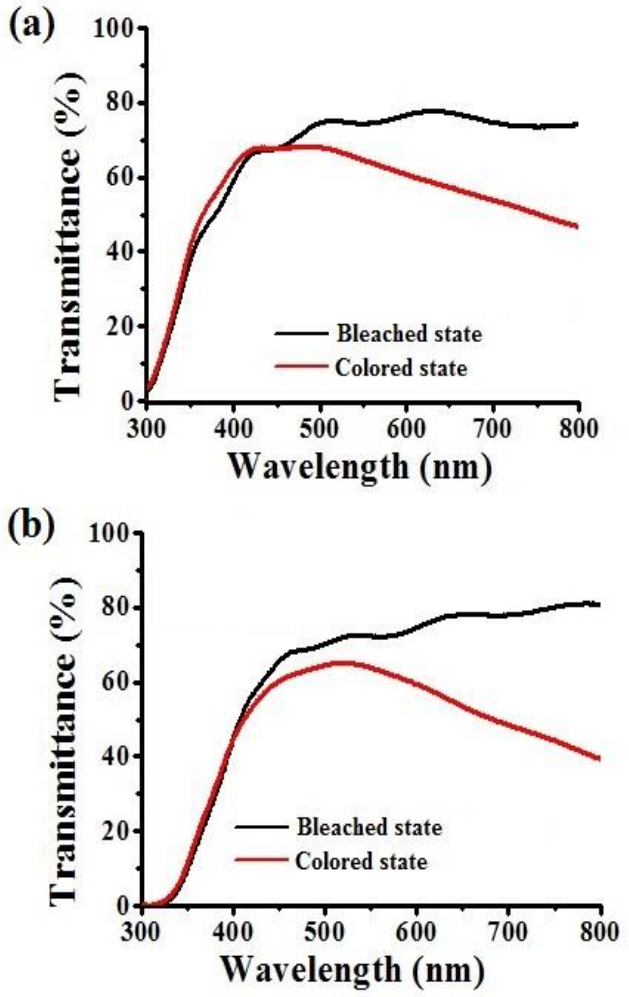

Fig. 6. Transmittance measurements of the WO_3 layers grown at various deposition temperatures: 450ºC (a) 550ºC (b).

From these graphs the change in optical density at 670nm can be estimated according to the equation:

$$\Delta(OD) = \log (Tb / Tc)$$

where Tb and Tc are the transmittance at bleached and colored state respectively. Then, the coloration efficiency can be determined using the equation:

$$\eta = \Delta(OD) / Qi$$

where Qi is the intercalation charge density [39]. The coloration efficiency for the deposition at 450 ºC was determined to be 32.5 cm^2 / C, while for the deposition at 550 ºC its value was slightly increased to 38.8 cm^2 / C, values in good agreement with the values reported [40-41]. The good electrochromic results combined with the one step process using a simple low cost deposition technic made the specific method attractive for large scale production.

Conclusion

Monoclinic tungsten trioxide layers were developed at various deposition temperatures, using a low pressure CVD system. It was found that the increase of the deposition temperature improves the crystallinity and modifies the preferred orientation of the as-grown layers. This affects the morphology of the layers, since, as the deposition temperature increases, the surface becoming more porous, which, in combination with the improved crystallinity, enlarges the intercalation charge, according the chronoamperometry measurements. The most stable layers was that deposited at 450ºC, since it combines good crystallinity, uniform surface and good stability during the cyclic voltammetry cycles.

Acknowledgements

The author would like to thanks the Greek State Scholarship Foundation (I.K.Y) for the partial financial support: IKY FELLOWSHIPS OF EXCELLENCE FOR POSTGRADUATE STUDIES IN GREECE - SIEMENS PROGRAM.

References

1. Talledo, A; Granqvist, C.G. Structural evolution during lithiation of sputtered V_2O_5 films. Appl. Phys. A **1995,** 60, 521 **DOI:** 10.1007/BF01538779
2. Wang, Y.; Cao, G. Synthesis and enhanced intercalation properties of nanostructured vanadium oxides. Chem. Mater. **2006**, 18, 2787 **DOI:** 10.1021/cm052765h
3. Lindström, R.; Maurice, V.; Groult, H.; Perrigaud, L.; Zanna, S.; Cohen, C.; Marcus, P. Li-intercalation behaviour of vanadium oxide thin film prepared by thermal oxidation of vanadium metal. Electrochim. Acta **2006**, 51, 5001 **DOI:** 10.1016/j.electacta.2006.01.049
4. Vernardou, D.; Pemble, M.E.; Sheel, D.W. The growth of thermochromic VO_2 films on glass by atmospheric-pressure CVD: a comparative study of precursors, CVD methodology, and substrates. Chem. Vapor Depos. **2006**, 12, 263 **DOI:** 10.1002/cvde.200506419
5. Manning, T.D.; Parkin, I.P.; Clark, R.J.H.; Sheel, D.; Pemble, M.E.; Vernardou, D. Intelligent window coatings: atmospheric pressure chemical vapour deposition of vanadium oxides. J. Mater. Chem. **2002**, 12, 2936. **DOI:** 10.1039/B205427M
6. Louloudakis, D.; Vernardou, D.; Spanakis, E.; Suchea M,; Kenanakis, G; Pemble, M; Savvakis, K.; Katsarakis, N.; Koudoumas, E.; Kiriakidis, G. Atmospheric pressure chemical vapor deposition of amorphous tungsten doped vanadium dioxide for smart window applications. Adv. Mater. Lett. **2016**, 7(3), 192 **DOI:** 10.5185/amlett.2016.6024
7. Chain, E. E. Optical properties of vanadium dioxide and vanadium pentoxide thin films. Appl. Opt., **1991**, 30, 2782 **DOI:** 10.1364/AO.30.002782
8. Vernardou, D.; Drosos, H.; Spanakis, E.; Koudoumas, E.; Savvakis, C.; Katsarakis, N. Electrochemical and photocatalytic properties of WO_3 coatings grown at low temperatures. J. Mater. Chem. **2011**, 21, 513 **DOI:** 10.1039/c0jm02413a
9. Li, W.-J.; Fu, Z.-W. Nanostructured WO_3 thin film as a new anode material for lithium-ion batteries. Appl. Surf. Sci. **2010**, 256, 2447 **DOI:** 10.1016/j.apsusc.2009.10.085
10. Li, X.-L.; Lou, T.-J.; Sun, X.-M.; Li, Y.-D. Highly sensitiveWO_3 hollow-sphere gas sensors. Inorg. Chem. **2004**, 43, 5442 **DOI:** 10.1021/ic049522w
11. Susanti, D.; Dwi Wibawa, R.N.; Tananta, L.; Purwaningsih, H.; Fajarin, R.; Endri Kusuma, G. The effect of calcination temperature on the capacitive properties of WO_3-based electrochemical capacitors synthesized via a sol-gel method. Front. Mater. Sci. **2013**, 7, 370 **DOI:** 10.1007/s11706-013-0220-x
12. Svensson, J.S.E.M.; Granqvist, C.G. Modulated transmittance and reflectance in crystalline electrochromic WO_3 films: theoretical limits. Appl. Phys. Lett. **1984**, 45, 828 **DOI:** 10.1063/1.95415
13. Niklasson G. A.; Granqvist, C. G. Electrochromics for smart windows: thin films of tungsten oxide and nickel oxide, and devices based on these. J. Mater. Chem. **2007**, 17, 127 **DOI:** 10.1039/B612174H
14. Rubin, M.; K. von Rottkay,; Wen, S.-J.; Özer, N.; Slack, J. Optical indices of lithiated electrochromic oxides. Sol. Energy Mater. Sol. Cells **1998**, 54, 49 **DOI:** 10.1016/S0927-0248(97)00222-5
15. Suda, Y.; Kawasaki, H.; Ohshima, T.; Yagyuu, Y. Characteristics of tungsten oxide thin films prepared on the flexible substrates using pulsed laser deposition. Thin Solid Films **2008**, 516, 4397 **DOI:** 10.1016/j.tsf.2007.10.023
16. Yous, B.; Robin, S.; Donnadieu, A.; Dufour, D.; Maillot, C.; Roulet, H.; Senemaud, C. Chemical vapor deposition of tungsten oxides: A comparative study by X-ray photoelectron spectroscopy, X-ray diffraction and reflection high energy electron diffraction. Mater. Res. Bull. **1984**, 19, 1349 **DOI:** 10.1016/0025-5408(84)90199-5
17. Ivanova, T.; Gesheva, K.A.; Popkirov, G.; Ganchev, M.; Tzvetkova, E. Electrochromic properties of atmospheric CVD MoO_3 and MoO_3–WO_3 films and their application in electrochromic devices. Mater. Sci. Eng. B **2005**, 119, 232 **DOI:** 10.1016/j.mseb.2004.12.084
18. Davazoglou D.; Donnadieu, A. Electrochromism in polycrystalline WO_3 thin films prepared by chemical vapour deposition at high temperature. Thin Solid Films **1988**, 164, 369 **DOI:** 10.1016/0040-6090(88)90164-2
19. Vernardou, D.; Psifis, K.; Louloudakis, D.; Papadimitropoulos, G.; Davazoglou. D.; Katsarakis N.; Koudoumas, E. Low Pressure CVD of ElectrochromicWO_3 at 400ºC. J. Electrochem. Soc. **2015**, 162 (9) H579-H582 (2015) **DOI:** 10.1149/2.0281509jes
20. Klinke, C.; Hannon, J. B.; Gignac, L.; Reuter, K.; Avouris, P. Tungsten Oxide Nanowire Growth by Chemically Induced Strain. J. Phys. Chem. B **2005**, 109, 17787 **DOI:** 10.1021/jp0533224
21. Davazoglou, D.; Moutsakis, A.; Valamontes, V.; Psycharis, V.; Tsamakis, D. Tungsten Oxide Thin Films Chemically Vapor Deposited at Low Pressure by $W(CO)_6$ Pyrolysis. J. Electrochem. Soc. **1997**, 144, 595 **DOI:** 10.1149/1.1837453
22. Vernardou, D.; Louloudakis, D.; Spanakis, E.; Katsarakis, N.; Koudoumas, E. Electrochemical properties of vanadium oxide coatings grown by hydrothermal synthesis on FTO substrates. New J. Chem. **2014**, 38, 1959 **DOI:** 10.1039/C3NJ00931A
23. Vernardou, D.; Apostolopoulou, M.; Louloudakis, D.; Katsarakis, N.; Koudoumas, E. Hydrothermal growth and characterization of shape-controlled $NH_4V_3O_8$. New J. Chem. **2014**, 38, 2098 **DOI:** 10.1039/C3NJ01446K
24. Vernardou, D.; Apostolopoulou, M.; Louloudakis, D.; Katsarakis, N.; Koudoumas, E. Hydrothermally grown β-V_2O_5 electrode at 95 °C. J. Colloid Interf. Sci. **2014**, 424, 1 **DOI:** 10.1016/j.jcis.2014.03.004
25. Vernardou, D.; Apostolopoulou, M.; Louloudakis, D.; Spanakis, E.; Katsarakis, N.; Koudoumas, E.; McGrath, J.; Pemble, M.E. Electrochemical properties of opal-V_6O_{13} composites. J. Alloys Compd. **2014**, 586, 621 **DOI:** 10.1016/j.jallcom.2013.10.151
26. Elangovan E.; Ramamurthi, K. Studies on micro-structural and electrical properties of spray-deposited fluorine-doped tin oxide thin films from low-cost precursor. Thin Solid Films **2005**, 476, 231 **DOI:** 10.1016/j.tsf.2004.09.022
27. Hu, X.; Ji, Q.; Hill, J. P.; Ariga, K. Large-scale synthesis of WOx–EDA nanobelts and their application as photoswitches. Cryst. Eng. Comm. **2011**, 13, 2237 **DOI:** 10.1039/C0CE00466A
28. Zhang, H.; Yao, M.; Bai, L.; Xiang, W.; Jin, H.; Lin, J.; Yuan, F. Synthesis of uniform octahedral tungsten trioxide by RF induction

thermal plasma and its application in gas sensing. Cryst. Eng. Comm. **2013**, 15, 1432
DOI: 10.1039/C2CE26514A

29. Lu, Z.; Kanan, S. M.; Tripp, C. P. Synthesis of high surface area monoclinic WO_3 particles using organic ligands and emulsion based methods. J. Mater. Chem. **2002**, 12, 983
DOI: 10.1039/B107993J
30. Pecquenard, B.; Lecacheaux, H.; Livage, L.; Julien, C. Orthorhombic WO_3 formed via a Ti-stabilized $WO_3.1/3H_2O$ phase. J. Solid State Chem. **1998**, 135, 159
DOI: 10.1006/jssc.1997.7618
31. Habazaki, H.; Hayashi, Y.; Konno, H.; Characterization of electrodeposited WO_3 films and its application to electrochemical wastewater treatment. Electrochim. Acta **2002**, 47, 4181
DOI: 10.1016/S0013-4686(02)00435-8
32. Ng, C. Y.; Razak K. A.; Lockman, Z. A WO_3 Nanoporous-Nanorod Film Formed by Hydrothermal Growth of Nanorods on Anodized Nanoporous Substrate. J. Electrochem. Soc. **2015**, 162, 9, E148
DOI: 10.1149/2.0561509jes
33. C. G. Granqvist, Handbook of Inorganic Electrochromic Materials, Elsevier, New York 1995
ISBN: 9780080532905
34. Wan, Y.; Wang, X.; Liu, S.; Li, Y.; Sun, H.; Wang, Q. Effect of electrochemical factors on formation and reduction of Silver Oxides. Int. J. Electrochem. Sci. **2013**, 8, 12837
DOI: http://www.electrochemsci.org/papers/vol8/81212837.pdf
35. Huang, K.; Jia, J.; Pan, Q.; Yang, F.; He, D. Optical, electrochemical and structural properties of long-term cycled tungsten oxide films prepared by sol–gel. Physica B **2007**, 396, 164
DOI: 10.1016/j.physb.2007.03.031
36. Vernardou, D.; Paterakis, P.; Drosos, H.; Spanakis, E.; Povey, I. M.; Pemble, M. E.; Koudoumas, E.; Katsarakis, N. A study of the electrochemical performance of vanadium oxide thin films grown by atmospheric pressure chemical vapour deposition. Sol. Energ. Mat. Sol. C. **2011**, 95, 2842
DOI: 10.1016/j.solmat.2011.05.046
37. Christou, K.; Louloudakis, D.; Vernardou, D.; Katsarakis, N.; Koudoumas, E. One-pot synthesis of WO_3 structures at 95ºC using HCl. J. Sol-Gel Sci. Techn. **2015**, 73, 520
DOI: 10.1007/s10971-014-3459-5
38. Zheng, F.; Man, W.; Guo, M.; Zhang M.; Zhen, Q. Effects of morphology, size and crystallinity on the electrochromic properties of nanostructured WO_3 films. CrystEngComm, **2015**, 17, 5440
DOI: 10.1039/C5CE00832H
39. Bathe S. R.; Patil, P. S. Electrochromic characteristics of fibrous reticulated WO_3 thin films prepared by pulsed spray pyrolysis technique. Sol. Energy Mater. Sol. Cells **2007**, 91, 1097
DOI: 10.1016/j.solmat.2007.03.005
40. Granqvist, C.G. Electrochromic tungsten oxide films: Review of progress 1993-1998. Sol. Energy Mater. Sol. Cells **2000**, 60, 201
DOI: 10.1016/S0927-0248(99)00088-4
41. Bathe S. R.; Patil, P. S. Electrochemical Behavior of TiO_2 Nanoparticle Doped WO_3 Thin Films, Journal of Materials **2014**, 2014, 642069
DOI: 10.1155/2014/642069

